

Chemical Modification of Polyisobutylene Succinimide Dispersants and Characterization of their Associative Properties

Solmaz Pirouz, Yulin Wang, J. Michael Chong, Jean Duhamel*

Waterloo Institute for Nanotechnology, Institute for Polymer Research, Department of
Chemistry, University of Waterloo, Waterloo, ON N2L 3G1, Canada

* To whom correspondence should be addressed.

ABSTRACT

The secondary amines found in *b*-PIBSI dispersants prepared by attaching two polyisobutylene chains to a polyamine core via two succinimide moieties were reacted with ethylene carbonate (EC). The reaction generated urethane bonds on the polyamine core to yield the modified *b*-PIBSI dispersants (*Mb*-PIBSI). Five dispersants were prepared by reacting two molar equivalents (m_{eq}) of polyisobutylene terminated at one end with a succinic anhydride moiety (PIBSA) with one m_{eq} of hexamethylenediamine (HMDA), diethylenetriamine (DETA), triethylenetetramine (TETA), tetraethylenepentamine (TEPA), and pentaethylenehexamine (PEHA) to yield the corresponding *b*-PIBSI dispersants. Characterization of the level of secondary amine modification for the *Mb*-PIBSI dispersants with traditional techniques such as FTIR and ^1H NMR spectroscopies was greatly complicated by interactions between the carbonyls of the succinimide groups and unreacted secondary amines of the *Mb*-PIBSI dispersants. Therefore, an alternative procedure was developed based on fluorescence quenching of the succinimides by secondary amines and urethane groups. The procedure took advantage of the fact that the succinimide fluorescence of the *Mb*-PIBSI dispersants was quenched much more efficiently by secondary amines than by the urethane groups that resulted from the EC modification of the amines. While EC modification did not proceed for *b*-PIBSI-DETA and *b*-PIBSI-TETA certainly due to steric hindrance, 60 and 70% of the secondary amines found in the longer polyamine core of *b*-PIBSI-TEPA and *b*-PIBSI-PEHA had reacted with EC as determined by the fluorescence quenching analysis. Furthermore, the ability of the *Mb*-PIBSI dispersants to adsorb at the surface of carbon black particles used as mimic of the carbonaceous particles typically found in engine oils was compared to that of their unmodified analogs.

INTRODUCTION

Dispersants have been extensively used as oil additives since the 1950s. They are designed to improve engine oil performance and decrease fuel consumption and pollution emission.¹⁻³ Their purpose is to decrease soot aggregation, a process that can thicken the oil to the point where it generates sludge that prevents the flow of oil. Soot and sludge are carbon-rich and/or metallic in nature and result from the incomplete oxidation of fuel during ignition. Soot or ultrafine particles (UFPs) are smaller than 100 nm in diameter, but they aggregate over time into large particles (LPs) with a diameter on the order of 1 μm to minimize exposure of their polar surface to the oil.^{4,5} The formation of LPs can cause engine failure through wear and oil blockage. Dispersants adsorb onto the surface of UFPs, stabilizing them by a steric or electrostatic mechanism which reduces the aggregation of UFPs into LPs.^{1,5,6}

Metallic and ashless dispersants are two types of commonly used oil additives. Metal-containing dispersants have a good dispersancy capacity but the presence of metals can lead to the production of insoluble solids upon degradation. These solid salts actually add to the sludge problem. The other type of dispersant is referred to as ashless dispersant. Unlike metallic dispersants, ashless dispersants do not leave any ashes or embers in the engine.¹ Polyisobutylene succinimide (PIBSI) dispersants are the most common ashless dispersants used in the oil industry today and they were initially developed in 1966.⁷⁻¹⁰ They are constituted of a polyamine head and PIB-stabilizing tail. For a given succinimide dispersant, a higher number of secondary amines in the polyamine head results in a better adsorption of the dispersant onto the polar surface of UFPs but the basic polyamine linker of PIBSI dispersants compromises their compatibility with the fluorocarbon elastomers that are used as engine seals and this issue represents a challenging problem to the industry.^{3,6,11,12}

A number of approaches have been introduced to reduce the basicity of dispersant amines such as their modification with boric acid or ethylene carbonate.¹²⁻¹⁴ Although such capping agents generally improve compatibility of the dispersants with engine seals and the other compounds of the oil formulation, capping makes the dispersants less efficient. The preparation of modified *bis*-polyisobutylene succinimide dispersants (*Mb*-PIBSI) begins by generating the non-modified PIBSI dispersant as follows. Reaction of a polyisobutylene chain terminated at one end with a succinic anhydride group (PIBSA)^{9,15-17} with a polyamine terminated at both ends with two primary amines in a 1:2 polyamine:PIBSA ratio generates *bis*-PIBSI (*b*-PIBSI) dispersants.^{18,19} The *b*-PIBSI dispersants can be post-modified with reactants such as boric acid or ethylene carbonate to generate *Mb*-PIBSI. While these reactions have been reported in the literature for decades, a recent report has established that characterization of *b*-PIBSI dispersants remains challenging with techniques based on FTIR or ¹H NMR spectroscopies due to complications caused by interactions generated between the succinimide groups and secondary amines of *b*-PIBSI dispersants.²⁰

Interestingly the same study also found that the inherent fluorescence of the succinimide groups in the *b*-PIBSI dispersants was efficiently quenched by secondary and tertiary amines, and that the quenching efficiency increased linearly with increasing number of secondary amines in the polyamine linker used to prepare the *b*-PIBSI dispersants. Since chemical post-modification of *b*-PIBSI dispersants is common practice in the oil additive industry, and considering the challenges associated with the characterization of the chemical composition of *b*-PIBSI dispersants with traditional techniques, this report investigates the extent to which fluorescence quenching of the succinimide groups found in *b*-PIBSI dispersants could provide information about the chemical composition of *Mb*-PIBSI dispersants. To this end, *Mb*-PIBSI dispersants were prepared by ethylene carbonate post-

modification of *b*-PIBSI dispersants and the ability of FTIR, ¹H NMR, and fluorescence at providing quantitative information about their chemical composition was assessed. In particular, fluorescence was used as an analytical method to characterize the level of modification of *Mb*-PIBSI dispersants in terms of the number of unreacted secondary amines per gram of dispersant. This characterization method took advantage of the fluorescence of the succinimide moieties found in the *Mb*-PIBSI dispersants and the fact that they are being quenched with a different efficiency by secondary amines and urethane groups.^{20,24-27}

The chemical composition and structure of the dispersants are known to influence the reduction in sludge formation. The adsorption isotherms analysis can provide information on how effectively different dispersants bind onto the surface of carbon black particles (CBPs) used as mimics of UFPs.^{18,21-23} The adsorption isotherms of a series of PIBSI dispersants have been determined in apolar hexane earlier and the results showed an increase in the association strength of the dispersant with increasing number of secondary amines in the polyamine core.¹⁸ The present study compares the adsorption isotherms in dodecane of *b*-PIBSI and *Mb*-PIBSI dispersants onto CBPs by using the inherent fluorescence of the succinimide groups. The results indicate that EC-post-modification of *b*-PIBSI dispersants lowers their ability to bind onto CBPs. It confirms that a trade-off must be reached between the reduction in secondary amine basicity through EC modification of *b*-PIBSI dispersants and their ability to latch onto the surface of UFPs.

EXPERIMENTAL

Chemicals. Acetone (HPLC grade, Caledon), hexane (HPLC grade, Caledon), xylene (reagent grade, 98.5%, EMD), deuterated chloroform (CDCl₃, 99.8%, Cambridge Isotope Laboratories, Inc.), tetrahydrofuran (THF, HPLC grade, Caledon), dodecane (anhydrous, 99%, Sigma-

Aldrich), ethyl ether (anhydrous, 99% Sigma-Aldrich), ethyl acetate (HPLC, 99.7% Sigma-Aldrich), and 2-dodecanone (GC grade, 97%, Sigma-Aldrich) were used as received. The chemicals hexamethylenediamine (HMDA, 98%), diethylenetriamine (DETA, 99%), triethylenetetramine (TETA, 97%), tetraethylenepentamine (TEPA, technical grade), pentaethylenehexamine (PEHA, technical grade), dibutylamine (DBA, 99.5%), octylamine (99%), *N*-methylsuccinimide (*N*-MSI, 99%), butylamine (BUA, 99%), diethylamine (DEA, 99.5%), triethylamine (TEA, 99.5%), ethylene carbonate (EC, 98%), magnesium sulfate anhydrous (97%), and activated charcoal (100 mesh) were purchased from Sigma-Aldrich and were employed without further purification. Polyisobutylene succinic anhydride (PIBSA) was supplied by Imperial Oil. The chemical composition of this sample was characterized by NMR, GPC, and FTIR analysis and found to contain on average one SA unit per 52 ± 2 isobutylene monomers. Assuming one SA moiety per chain, this PIBSA sample would have an M_n of $3,012 \text{ g}\cdot\text{mol}^{-1}$ equivalent to a total acid number (TAN) of 37.2 mg of KOH per gram of PIBSA.

Proton Nuclear Magnetic Resonance (^1H NMR). A Bruker 300 MHz high resolution NMR spectrometer was used to acquire the ^1H NMR spectra with a polymer concentration of about 10 mg/mL in CDCl_3 .

Fourier Transform Infrared (FTIR). A Bruker Tensor 27 FTIR spectrometer was used to acquire all FTIR spectra with an absorbance smaller than unity to avoid saturation of the detector. Polymer solutions prepared in CDCl_3 were deposited drop wisely onto the NaCl FTIR cell. The solvent was evaporated under a stream of nitrogen leaving behind a thin polymer film.

UV-Visible Spectrophotometer. Absorbance measurements were conducted on a Cary 100 UV-Visible spectrophotometer. Absorption spectra were acquired between 200 and 600 nm with quartz cells having path lengths of 0.1, 1, or 10 mm.

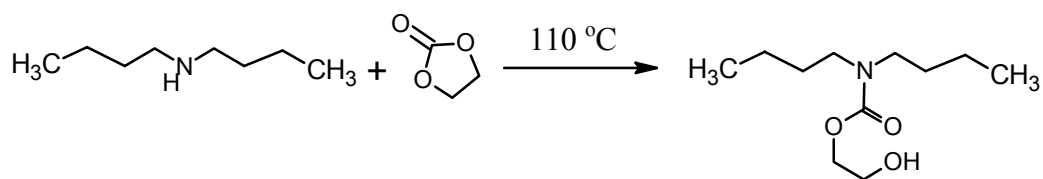
Steady-State Fluorescence. A Photon Technology International (PTI) LS-100 steady-state fluorometer was used to acquire the fluorescence spectra. The instrument was equipped with an Ushio UXL-75Xe Xenon arc lamp and a PTI 814 photomultiplier detection system. The emission spectra were excited at 360 nm and acquired from 365 to 600 nm.

Time-Resolved Fluorescence. All solutions were excited at 360 nm with a 340 nano-LED light source fitted onto an IBH time-resolved fluorometer to acquire their fluorescence decays at 428 nm. Fluorescence decay analysis included light scattering and background corrections. The sum of exponentials shown in Equation 1 was applied to fit the fluorescence decays of the *b*-PIBSI dispersants.

$$i(t) = \sum_{i=1}^{n_{\text{exp}}} a_i \times \exp(-t / \tau_i) \quad (1)$$

In Equation 1, n_{exp} represents the number of exponentials used in the decay analysis and the parameters a_i and τ_i represent the amplitude and decay time of the i^{th} exponential, respectively. The decay fits were deemed satisfactory if the χ^2 value was smaller than 1.30 and the residuals and the autocorrelation of the residuals were randomly distributed around zero.

Synthesis of 2-Hydroxyethyl *N,N*-Dibutylcarbamate. 2-Hydroxyethyl *N,N*-dibutylcarbamate (HEDBC) was prepared by reacting one molar equivalent of dibutylamine (DBA) with a slight excess of ethylene carbonate (EC) according to Scheme 1.



Scheme 1. Reaction of dibutylamine (DBA) and ethylene carbonate (EC).

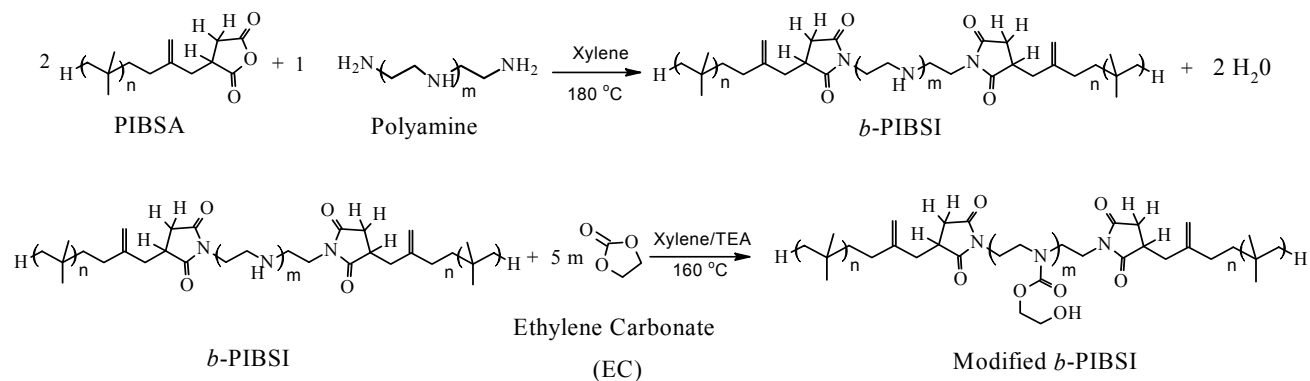
DBA (4.0 g, 31 mmol) and EC (2.8 g, 32 mmol) were added in a two neck round bottom flask capped with a water condenser. The reaction was carried out without solvent under nitrogen at 110 °C for 20 hours. The product mixture was dissolved in 100 mL of diethyl ether and extracted with 100 mL of HCl (1 M) solution. Unreacted EC partitioned into the aqueous layer whereas the carbamate products stayed in the organic layer. Magnesium sulfate anhydrous was used to dry the ether fraction and was removed by filtration. Column chromatography with silica gel was performed to isolate the desired product. A 1:1 ratio of hexane and ethyl acetate solution was used as the eluent and the products were separated. Three different compounds were found in the organic layer. The ^1H NMR spectrum of the desired compound obtained after separation via column chromatography is shown as supporting information (SI) in Figure S1.

Comparison of the spectra of DBA and HEDBC indicates that the peak of the methylene protons **1** of the butyl groups next to the nitrogen shifted from 2.5 to 3.15 ppm. Proton **1** of HEDBC is also broader due to hindered rotation about the C-N bond of the carbamate group in HEDBC. New peaks appeared at 2.8, 3.8, and 4.2 ppm. The triplet at 2.8 ppm represented the alcohol proton while the peaks at 3.8 and 4.2 ppm were assigned to the methylene protons α and β to the alcohol, respectively.

Synthesis of the Polyisobutylene Succinimide (PIBSI) Dispersants. The polyisobutylene succinimide (*b*-PIBSI) dispersants were prepared from the reaction of one molar equivalent (m_{eq}) of different polyamine derivatives with two m_{eq} of PIBSA as described in Scheme 2. In the current study, hexamethylenediamine (HMDA), diethylenetriamine (DETA), triethylenetetramine (TETA), tetraethylenepentamine (TEPA), and pentaethylenehexamine (PEHA) were used as polyamines and their chemical structure is given in Table 1. All *b*-PIBSI dispersants were synthesized according to Scheme 2 based on a procedure that has been described in detail in an earlier publication.^{18,20}

Table 1. Chemical structures of the amine derivatives used to prepare the *b*-PIBSI dispersants.

Polyamine	Chemical Structure
Hexamethylenediamine (HMDA)	$H_2N-(CH_2CH_2)_3-NH_2$
Diethylenetriamine (DETA)	$H_2N-(CH_2CH_2-NH)_2-H$
Triethylenetetramine (TETA)	$H_2N-(CH_2CH_2-NH)_3-H$
Tetraethylenepentamine (TEPA)	$H_2N-(CH_2CH_2-NH)_4-H$
Pentaethylenehexamine (PEHA)	$H_2N-(CH_2CH_2-NH)_5-H$



Scheme 2. Synthesis and modification of succinimide dispersants.

Successful reaction was confirmed by comparison of the FTIR absorption of dehydrated PIBSA (Trace A) with that of the *b*-PIBSI dispersant (Trace B) in Figure 1. PIBSA was dehydrated before the reaction since SA is much more reactive than succinic acid toward the nucleophilic attack by the primary amine end-groups of the polyamines. The FTIR spectrum of PIBSA shows an absorption band at 1785 cm^{-1} due to the carbonyl groups of succinic anhydride (SA). After reaction, the absorption at 1785 cm^{-1} disappeared and a new peak appeared at 1705 cm^{-1} in Trace B due to the succinimide carbonyls.

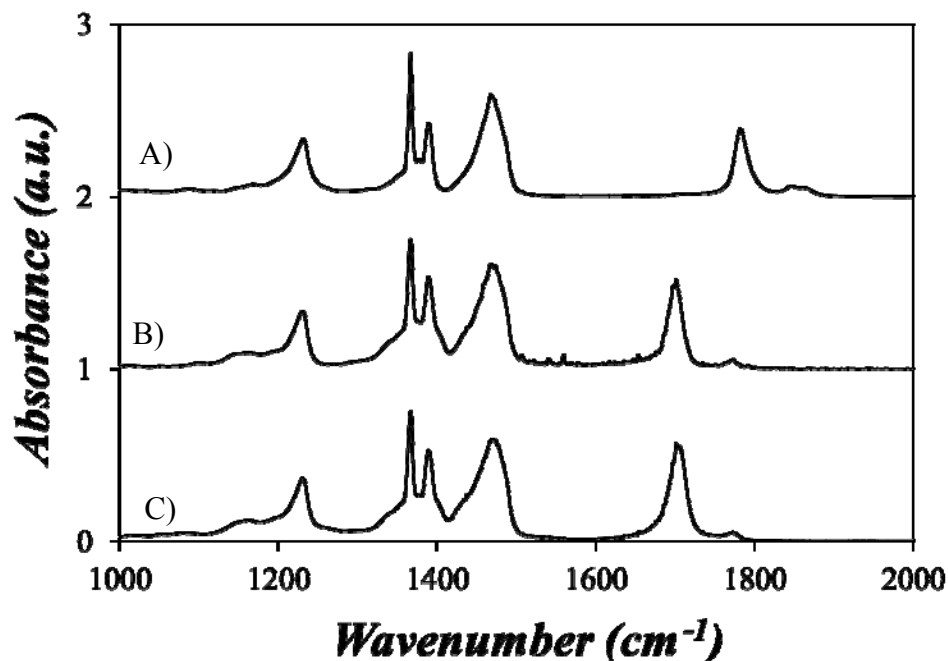


Figure 1. FT-IR spectra of A) dehydrated PIBSA, B) *b*-PIBSI-PEHA, and C) *Mb*-PIBSI-PEHA.

Modification of the Polyisobutylene Succinimide (*Mb*-PIBSI) Dispersants. The post-modification of all *b*-PIBSI dispersants was conducted in the same manner and is described in detail for *b*-PIBSI-PEHA. *b*-PIBSI-PEHA (0.50 g, 77 μmol) and EC (0.14 g, 1.54 mmol) were mixed with a 1:5 excess molar ratio of secondary amines-to-EC. The mixture was then dissolved in xylene (1.00 g, 1.14 mL) and TEA (0.50 g, 0.69 mL). The modification reaction was carried out in a sealed reaction vessel since EC tends to evaporate at the temperature used for the modification reaction. Furthermore, the reaction mixture was degassed with nitrogen for 15 minutes before the reaction and after each sampling of the reaction mixture made to monitor the reaction progress. After degassing, the mixture was heated to 160 $^{\circ}\text{C}$ and kept at this temperature for 24 h. Aliquots were withdrawn over time through a rubber septum tightly fastened to the reaction vessel to follow the reaction progress. After completion, the reaction

product was washed with 20 mL of distilled water three times. Finally the product was dried in a vacuum oven at 70 °C overnight. The main features of its FTIR spectrum shown as Trace C in Figure 1 will be discussed later.

Gel Permeation Chromatography (GPC). A Viscotek GPC max VE 2001 instrument equipped with a Viscotek TDA 305 triple detector array comprised of a refractive index, viscosity, and light scattering detector was used. The samples were passed through a divinylbenzene mixed bed Polyanalytik column. Tetrahydrofuran (THF) was used as the solvent at a flow rate of 1.0 mL/min. All samples were filtered using a 0.2 µm Millipore polytetrafluoroethylene (PTFE) filter before injection and the sample concentration was less than 10 mg/mL. Due to their low molecular weight ($< 6,000 \text{ g}\cdot\text{mol}^{-1}$), the polyisobutylene samples used in this study did not scatter light strongly enough to yield a reliable light scattering signal and the light scattering detector of the GPC instrument could not be used to determine their absolute molecular weight. Instead the GPC instrument determined the apparent molecular weight of the polyisobutylene samples as it was calibrated with polystyrene standards.

The GPC trace obtained for PIBSA, *b*-PIBSI-PEHA, and *Mb*-PIBSI-PEHA are shown in Figure S2. PIBSA eluted at an elution volume (V_{el}) of 25 mL. GPC analysis of the product of the reaction between 1 molar equivalent (m_{eq}) of a polyamine like PEHA and 2 m_{eq} of PIBSA yielded a main peak in Figure S2 that was shifted to a lower elution volume ($V_{el} = 23 \text{ mL}$) compared to PIBSA reflecting the expected increase in molecular weight. From the overlaying of the GPC traces obtained for *b*-PIBSI-PEHA (trace B) and *Mb*-PIBSI-PEHA (trace C) in Figure S2, it could be concluded that modification of the PIBSI dispersants with EC did not affect their molecular weight distribution.

RESULTS AND DISCUSSION

Proton Nuclear Magnetic Resonance (^1H NMR). PIBSA was used as the starting material in the synthesis of *Mb*-PIBSI. PIBSA was reacted with DETA, TETA, TEPA, and PEHA to produce a series of *b*-PIBSI dispersants which were post-modified with EC to generate *Mb*-PIBSI. The ^1H NMR spectra of PIBSA, *b*-PIBSI-TEPA, and *Mb*-PIBSI-TEPA are shown in Figure S3. In the spectrum of PIBSA presented in Figure S3A, the peaks at 2.6 and 3.3 ppm represent the protons in the succinic anhydride ring. After reaction with a polyamine, these peaks shifted to 2.5 and 3.0 ppm in Figure S3B, and new peaks appeared at 2.8 and 3.5 ppm representing the ethylene protons in the polar core of the *b*-PIBSI dispersant. In all polymer samples, the peaks at 1.1 and 1.4 ppm (not shown in Figure S3) represent, respectively, the methylene and the methyl protons of the PIB backbone obtained in a 1:3 ratio. The peak at 5.5 ppm was found for all polymer samples and might be due to the presence of vinyl groups generated during the Alder-ene reaction of PIBSA as inferred from a detailed NMR characterization of PIBSA samples.¹⁷ The sharp peaks at 2.25 and 2.3 ppm in Figure S3C are due to traces of xylene. The assignment of the ^1H NMR spectrum of *Mb*-PIBSI-TEPA (Figure S3C) was done by comparing it to that of HEDBC (Figure S1). The two peaks at 3.8 and 4.2 ppm found in the ^1H NMR spectrum of *Mb*-PIBSI-TEPA correspond to the methylene protons in the carbamate side chain, with a same chemical shift as that found in the ^1H NMR spectrum of HEDBC in Figure S1. In the spectrum of *Mb*-PIBSI-TEPA, the peak at 2.8 ppm was reduced and the peak at 3.5 ppm was enlarged as the environment of the methylene protons in the α position to the central carbamate became similar to that of the methylene protons in the α position to the succinimide groups. Based on ^1H NMR, modification of *b*-PIBSI-DETA and *b*-PIBSI-TETA was inefficient, showing no peak at 3.8 and 4.2 ppm after

reaction with EC as shown in Figures S4A and S4B. The fact that modification was successful with *b*-PIBSI-TEPA and *b*-PIBSI-PEHA (Figures S4C and S4D) which both have a longer, and thus more accessible, polyamine spacer suggests that the absence of reaction observed with *b*-PIBSI dispersants having a shorter linker might be the result of steric hindrance.

In an ideal case, when all secondary amines have reacted, ¹H NMR spectroscopy can be used to determine the exact yield of the modified dispersants. But in practice, there remain some unreacted secondary amines in the polyamine linker that might cause aggregation due to H-bonding between the secondary amine protons and the succinimide carbonyls, and lead to distortion by broadening of the ¹H NMR peaks due to slower tumbling. Equation 2 was applied to calculate the modification yield of *b*-PIBSI dispersants by using the number of urethane moieties (N_{UR}) generated in the polyamine linker per number of isobutylene monomers (N_{IB}).

$$Yield\% = \frac{\left(\frac{N_{UR}}{N_{IB}}\right)_{\text{Real}}}{\left(\frac{N_{UR}}{N_{IB}}\right)_{\text{Ideal}}} \quad (2)$$

According to our previous paper,²⁰ the ratio of succinimide moiety to N_{IB} in a *b*-PIBSI molecule equals 1:52 for *b*-PIBSI dispersants, but distortion of the ¹H NMR spectra due to aggregation of the dispersants resulted in an apparent 1:32 ratio based on integration of the ¹H NMR peaks. Thus $(N_{UR}/N_{IB})_{\text{Ideal}}$ in Equation 2 equals $\frac{m}{2}(N_{SI}/N_{IB})$ where m represents the number of secondary amines in the polymer linker and N_{SI}/N_{IB} equals 1:52 or 1:32 assuming that aggregation of the dispersants does not or does occur, respectively. Assuming no aggregation, reaction yields of $106 \pm 2\%$ and $95 \pm 1\%$ were calculated for *Mb*-PIBSI-TEPA

and *Mb*-PIBSI-PEHA, respectively, suggesting complete modification of the secondary amines of the polyamine linker. On the other hand, reaction yields of $66 \pm 2 \%$ and $62 \pm 2 \%$ were calculated for *Mb*-PIBSI-TEPA and *Mb*-PIBSI-PEHA, respectively, assuming aggregation of the dispersant and using the apparent N_{SI}/N_{IB} ratio equal to 1:32. As it turns out, fluorescence quenching experiments described later on demonstrate unambiguously that complete modification of the secondary amines did not occur, but that partial modification of the secondary amines took place in a proportion similar to what was determined by ^1H NMR assuming aggregation of the modified dispersants.

Fourier Transform Infrared (FTIR). FTIR spectra were obtained for the *b*-PIBSI and *Mb*-PIBSI dispersants. The peak at 1705 cm^{-1} characteristic of the succinimide or carbamate carbonyls was monitored in terms of its band intensity I_{max} (with respect to the signal at 1390 cm^{-1}) and full width at half maximum (FWHM). The results presented in Table 2 showed that *b*-PIBSI-DETA, *b*-PIBSI-TETA, *b*-PIBSI-TEPA, and *b*-PIBSI-PEHA have a larger I_{max} and FWHM in comparison to *b*-PIBSI-HMDA due to intermolecular aggregation induced by H-bonding between the secondary amines of the spacer and the succinimide carbonyls (Figure 1 and Table 2).²⁰ Furthermore, the FTIR results for *Mb*-PIBSI-DETA and *Mb*-PIBSI-TETA did not show any changes in I_{max} and FWHM within experimental error when compared to their unmodified analogs as expected since ^1H NMR analysis indicated that EC modification did not proceed with these two samples. The FTIR results for *Mb*-PIBSI-TEPA and *Mb*-PIBSI-PEHA indicated that I_{max} and FWHM for the peak at 1705 cm^{-1} became larger after modification (Figure 1 and Table 2). This analysis confirmed the successful modification of the *b*-PIBSI dispersants prepared with a longer polyamine linker observed by ^1H NMR. The increase in I_{max} and FWHM results from the increased number of carbonyl groups found in

the polar core of these dispersants after EC modification. The summary of the I_{\max} and FWHM values for the *b*-PIBSI dispersants before and after modification is shown in Table 2.

Table 2. Maximum peak intensity ($\frac{I_{\max}(1705\text{ cm}^{-1})}{I_{\max}(1390\text{ cm}^{-1})}$) and full width half max (FWHM) values calculated from FTIR spectrum.

Polymer	$\frac{I_{\max}(1705\text{ cm}^{-1})}{I_{\max}(1390\text{ cm}^{-1})}$	FWHM	Polymer	$\frac{I_{\max}(1705\text{ cm}^{-1})}{I_{\max}(1390\text{ cm}^{-1})}$	FWHM
<i>b</i> -PIBSI-HMDA	0.35	13			
<i>b</i> -PIBSI-DETA	0.54	14	<i>Mb</i> -PIBSI-DETA	0.49	15
<i>b</i> -PIBSI-TETA	0.53	16	<i>Mb</i> -PIBSI-TETA	0.51	16
<i>b</i> -PIBSI-TEPA	0.49	16	<i>Mb</i> -PIBSI-TEPA	0.64	26
<i>b</i> -PIBSI-PEHA	0.52	20	<i>Mb</i> -PIBSI-PEHA	0.65	35

Steady-State and Time-Resolved Fluorescence Measurements. Fluorescence was applied to estimate the level of modification of the *Mb*-PIBSI dispersants. The intrinsic fluorescence of the succinimide groups has been shown to be efficiently quenched by the secondary amines of the polyamine spacer of *b*-PIBSI dispersants.²⁰ Since the EC modification of PIBSI dispersants replaces the secondary amines of the *b*-PIBSI polyamine linker by urethane functions, the ability of a urethane group to quench the fluorescence of succinimide moieties was determined by monitoring the fluorescence of *N*-methylsuccinimide (*N*-MSI) as a function of 2-hydroxyethyl *N,N*-dibutylcarbamate (HEDBC) concentration in THF. Figure 2A for the steady-state fluorescence spectra and Figure 2B for the time-resolved fluorescence decays showed that addition of up to 0.3 M HEDBC to the *N*-MSI solution resulted in a smaller than 50% decrease in the fluorescence intensity (I) and number average lifetime $\langle \tau \rangle$.²⁰ By comparison, quenching of the fluorescence of *N*-MSI by 0.3 M diethylamine (DEA)

would have resulted in a much more pronounced 88% decrease in I and a 78% reduction in $\langle\tau\rangle$.²⁰ The pre-exponential factors and decay times retrieved from the multiexponential analysis of the fluorescence decays are reported in Table S1 in SI. The spectra and decays shown in Figures 2A and 2B were then used to determine the ratios I_0/I and $\langle\tau\rangle_0/\langle\tau\rangle$ which were then plotted as a function of HEDBC concentration in Figure 2C. I_0 and $\langle\tau\rangle_0$ represent the fluorescence intensity and number average lifetime of *N*-MSI in the absence of HEDBC. The trends obtained in Figure 2C with I_0/I and $\langle\tau\rangle_0/\langle\tau\rangle$ yield similar straight lines which suggested that little static quenching occurred contrary to what was observed for the quenching of *N*-MSI by DEA.²⁰ The similar lines observed for the I_0/I and $\langle\tau\rangle_0/\langle\tau\rangle$ trends reflect the absence of static quenching and thus aggregation between MSI and HEDBC. It also indicates that the propensity of the hydroxyl proton of HEDBC to H-bond with the carbonyls of *N*-MSI is much weaker than the amine proton of DEA. The slope obtained for $\langle\tau\rangle_0/\langle\tau\rangle$ in Figure 2C can be used to determine the quenching rate constant (k_Q) found to equal $2.5 \pm 0.2 \times 10^8 \text{ M}^{-1} \cdot \text{s}^{-1}$, 7 times smaller than the k_Q value of $17.4 \pm 0.2 \times 10^8 \text{ M}^{-1} \cdot \text{s}^{-1}$ obtained for the quenching of *N*-MSI by DEA indicating that the urethane moiety of HEDBC constitutes a much weaker quencher for *N*-MSI compared to the secondary amine of DEA. The substantial reduction in quenching observed from DEA to HEDBC should lead to obvious changes in the fluorescence response of the succinimide moieties found in the *b*-PIBSI dispersants after modification of their secondary amines by EC.

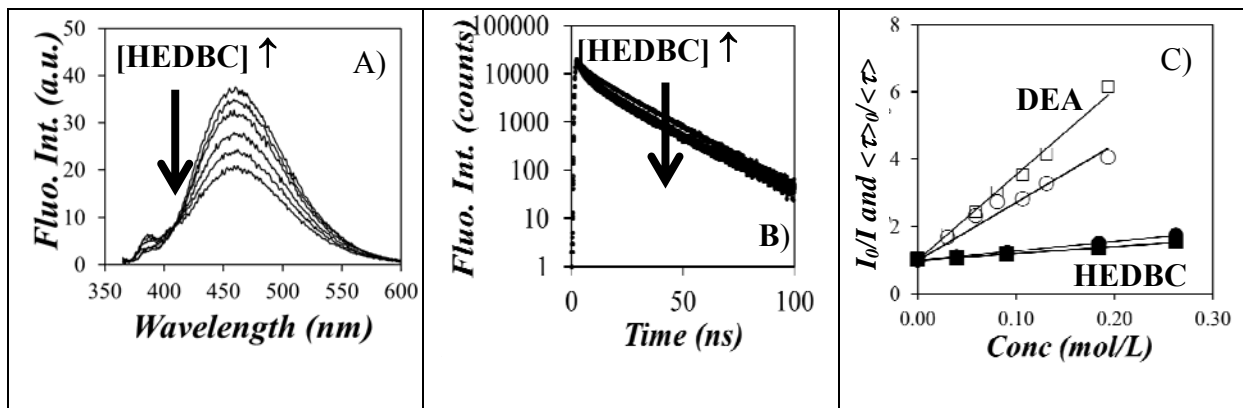


Figure 2. A) Steady-state fluorescence spectra and B) fluorescence decay of *N*-MSI quenched with HEDBC in THF. C) Stern-Volmer plot for the quenching of *N*-MSI with HEDBC (\blacksquare) I_0/I and (\bullet) $\langle \tau \rangle_0 / \langle \tau \rangle$ and DEA (\square) I_0/I and (\circ) $\langle \tau \rangle_0 / \langle \tau \rangle$ in THF. From top to bottom: The HEDBC concentrations in Figure 2A and 2B varied from 0 M to 0.3 M. ($C_{N-MSI} = 0.45$ mol/L, $\lambda_{ex} = 360$ nm, $\lambda_{em} = 428$ nm).

This was indeed observed in Figures 3A and B where the fluorescence intensity increased after modification of the *b*-PIBSI dispersants with EC. Beside transforming the strongly quenching secondary amines into weakly quenching urethanes, EC modification of the secondary amines of the *b*-PIBSI dispersants strongly reduced the ability of the *Mb*-PIBSI dispersants to aggregate, and thus the ability of the unreacted secondary amines to quench the fluorescence of the SI units of the dispersants. These combined effects associated with EC modification led to the partial recovery of the fluorescence of the SI units in Figures 3A and B. However the increase in fluorescence intensity shown in Figures 3A and B was quite minor compared to what would have been expected based on the reduction in fluorescence quenching observed in Figure 2C upon replacing a secondary amine by a urethane group. In fact, the complete modification of the secondary amines in the linker into urethane groups should have resulted in an increase in the fluorescence intensity of *Mb*-PIBSI-TEPA and

Mb-PIBSI-PEHA corresponding to 81% and 77% of the fluorescence intensity of *b*-PIBSI-HMDA shown as a reference in Figure 3. The fact that this was not observed led to the conclusion that not all secondary amines in *b*-PIBSI-TEPA and *b*-PIBSI-PEHA had been modified upon reaction with EC. This conclusion was further supported from the visual inspection of the fluorescence decays of *Mb*-PIBSI-TEPA and *Mb*-PIBSI-PEHA which showed hardly any difference with the dispersants before modification.

The fluorescence spectra and decays shown in Figures 3A–D were analyzed to determine the corresponding fluorescence intensity I and number average lifetime $\langle \tau \rangle$ for *Mb*-PIBSI-TEPA and *Mb*-PIBSI-PEHA. The pre-exponential factors and decay times retrieved from the decay analysis have been listed in Table S2. Using *b*-PIBSI-HMDA as a reference for the I_0 and $\langle \tau \rangle_0$ values of unquenched succinimide groups in *b*-PIBSI dispersants as done in an earlier publication,²⁰ the ratios I_0/I and $\langle \tau \rangle_0/\langle \tau \rangle$ for the two modified dispersants were plotted in Figure 4 as a function of the number of secondary amines in the linker, along the I_0/I and $\langle \tau \rangle_0/\langle \tau \rangle$ ratios which were obtained earlier for the unmodified dispersants *b*-PIBSI-DETA, *b*-PIBSI-TETA, *b*-PIBSI-TEPA, and *b*-PIBSI-PEHA.²⁰ The same trends were obtained in dodecane, THF, and dodecanone. The $\langle \tau \rangle_0/\langle \tau \rangle$ ratios showed minor differences for the dispersants before and after modification. The I_0/I ratios showed more substantial changes but took values that were much larger than unity contrary to what was expected if the EC modification had been complete.

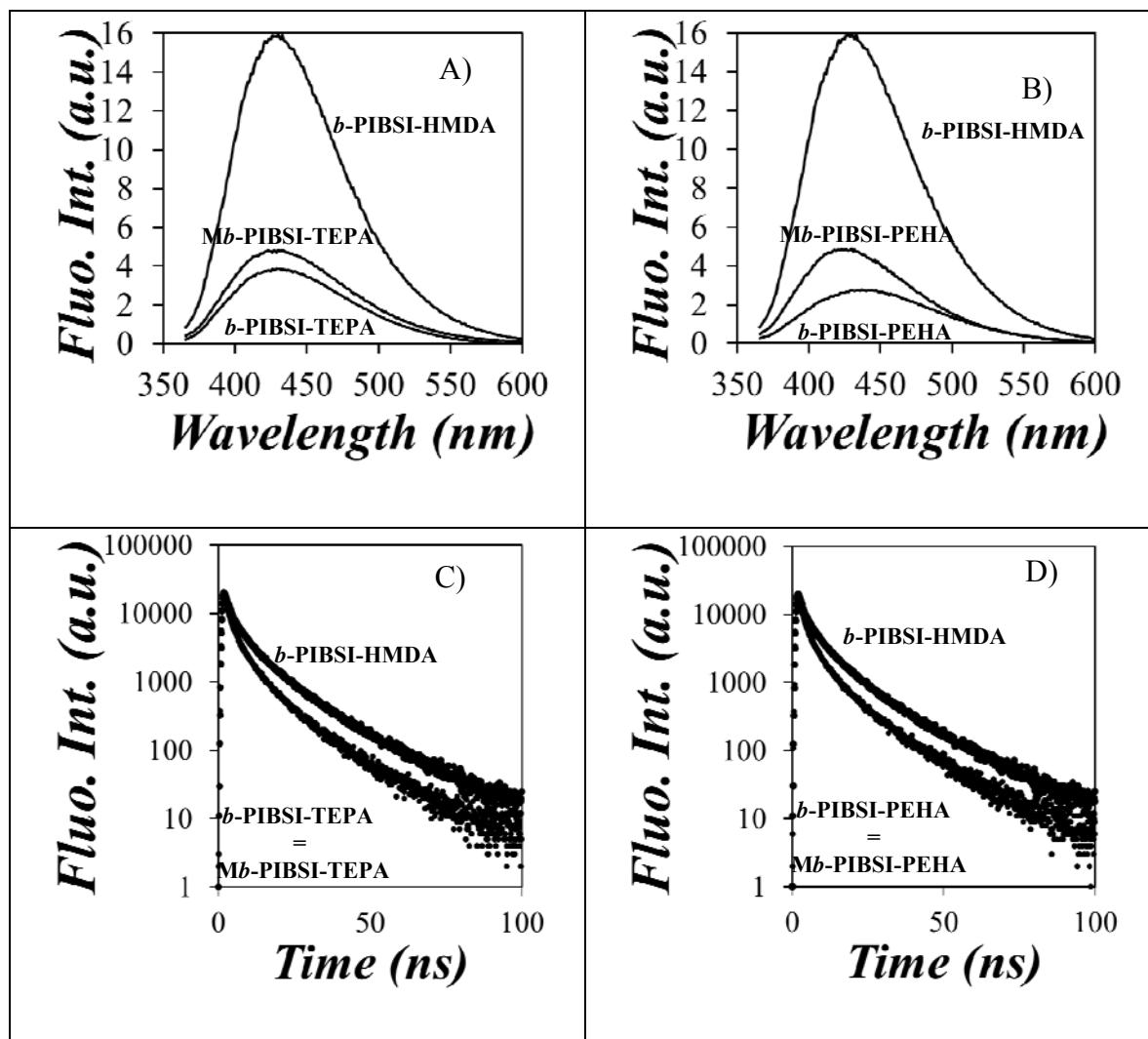


Figure 3. Steady-state fluorescence spectra (A and B) and time-resolved fluorescence decays (C and D). From top to bottom A) and C): *b*-PIBSI-HMDA, *Mb*-PIBSI-TEPA, and *b*-PIBSI-TEPA dispersants in dodecane and B) and D): *b*-PIBSI-HMDA, *Mb*-PIBSI-PEHA, and *b*-PIBSI-PEHA dispersants in dodecane. ($\lambda_{\text{ex}} = 360 \text{ nm}$, $\lambda_{\text{em}} = 428 \text{ nm}$)

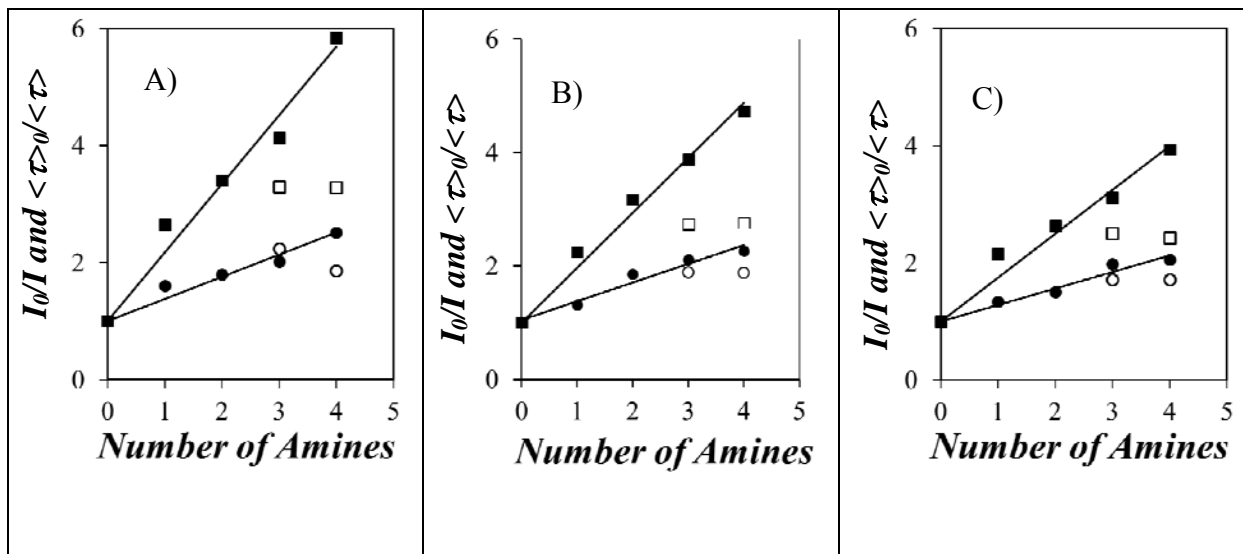


Figure 4. (●) I_0/I and (■) $\langle \tau \rangle_0 / \langle \tau \rangle$ of *b*-PIBSI dispersants and (○) I_0/I and (□) $\langle \tau \rangle_0 / \langle \tau \rangle$ of *Mb*-PIBSI dispersants versus number of secondary amines, in A) dodecane, B) THF, C) dodecanone.

The poor recovery in fluorescence signal observed after the EC modification of the polyamine linkers was attributed to the incomplete transformation of the secondary amines in the linker into urethane groups. In turn, the unreacted secondary amines could H-bond effectively with the carbonyls of the succinimide and urethane groups, resulting in a substantial static quenching as observed from the different I_0/I and $\langle \tau \rangle_0 / \langle \tau \rangle$ ratios. The I_0/I ratio probes both the static and dynamic quenching of the succinimide groups and its expression is provided in Equation 3. Because I_0/I responds to both types of quenching, it is much more sensitive than the ratio $\langle \tau \rangle_0 / \langle \tau \rangle$ that is influenced by dynamic quenching only. Therefore, the I_0/I ratio was selected to probe the effect that EC modification of the PIBSI secondary amines would have on the efficiency of quenching.

$$\frac{I_0}{I} = 1 + (\alpha K_{SV} [Q]_0 + (1 - \alpha) K_{SV}^M [Q]_0) \quad (3)$$

In Equation 3, I_0 and I represent the fluorescence intensity of *b*-PIBSI-HMDA and that of the modified dispersants, respectively. The constants K_{SV} ($= K_S + K_D$) and K_{SV}^M are the Stern-Volmer constants resulting from dynamic (K_D) and static quenching (K_S) of the unmodified and modified dispersants, respectively. $[Q]_0$ corresponds to the local concentration of secondary amines in the unmodified *b*-PIBSI dispersant and is equal to m/V_{core} where m and V_{core} are, respectively, the number of secondary amines (m) in the polyamine spacer of the dispersant and the core volume (V_{core}) which is assumed to be the same for our dispersants. The fraction α represents the molar fraction of unreacted secondary amines in the polyamine linker remaining after EC modification. The fraction α after EC modification was retrieved by rearranging Equation 3 into Equation 4.

$$\frac{I_0}{I} - 1 = \frac{K_{SV}}{V_{core}} m (\alpha + (1 - \alpha) \frac{K_{SV}^M}{K_{SV}}) = \frac{K_{SV}}{V_{core}} m (\alpha + (1 - \alpha) K') \quad (4)$$

In Equation 4, $\frac{K_{SV}}{V_{core}}$ is the slope of the plot I_0/I versus the number of amines obtained for unmodified dispersants shown in Figure 4. $\frac{K_{SV}}{V_{core}}$ was found to equal 0.96 ± 0.01 for the *b*-PIBSI dispersants in THF, but the ratio $\frac{K_{SV}^M}{K_{SV}}$ in Equation 4 is unknown. Therefore, K' whose expression is given in Equation 5 was used to calculate α . K' can be approximated by taking the ratio of K_{SV}^{HEDBC} for HEDBC to K_{SV}^{DEA} for DEA obtained in THF whose values

have been listed in Table 3. This derivation takes advantage of the similarity in chemical composition between DEA and the secondary amines in the polyamine linker of the *b*-PIBSI dispersants on the one hand and between HEDBC and the urethane groups on the other hand. Based on the data listed in Table 3, the K' value was found to equal 0.079 ± 0.001 .

$$K' = \frac{K_{SV}^M}{K_{SV}} = \frac{K_{SV}^{HEDBC}}{K_{SV}^{DEA}} \quad (5)$$

Table 3. K_{SV} constants obtained from Stern-Volmer plot resulting from quenching of *N*-MSI by DEA, TEA, and HEDBC in THF.

Name	K_{SV} (M^{-1})
DEA	25.17 ± 0.01
TEA	25.08 ± 0.02
HEDBC	1.98 ± 0.02

Application of this procedure to the I_0/I ratios shown in Figure 4 for *Mb*-PIBSI-TEPA and *Mb*-PIBSI-PEHA yielded an α value in Equation 4 of 0.4 and 0.3, respectively, suggesting that 60 ± 1 and 70 ± 1 % of the secondary amines had reacted (Table 4). Incidentally, this conclusion agrees remarkably well with the findings by 1H NMR that 66 ± 2 and 62 ± 2 % of all secondary amines in the polyamine linker of, respectively, *Mb*-PIBSI-TEPA and *Mb*-PIBSI-PEHA had reacted when assuming that dispersant association took place in solution and assuming an apparent N_{SI}/N_{IB} ratio of 1:32. The fact that none of the one and two secondary amines in the linker of, respectively, *b*-PIBSI-DETA and *b*-PIBSI-TETA reacted with EC, and that about one of the three secondary amines of *b*-PIBSI-TEPA and one of the four secondary amines of *b*-PIBSI-PEHA did not react with EC strongly suggests that steric hindrance as well as H-bonding with succinimide carbonyls must contribute to lowering

the extent of EC modification. This conclusion agrees with all experimental evidence obtained thus far such as the difficulty in using ^1H NMR and FTIR to determine the extent of modification in the *Mb*-PIBSI dispersants due to the existence of strong H-bonds, and the fluorescence quenching experiments that clearly demonstrate that not all secondary amines have reacted with EC. The higher reactivity of the secondary amines of *Mb*-PIBSI-PEHA is attributed to their better accessibility to, and thus better reactivity with EC.

Table 4. Number of unreacted secondary amines and level of modification for *Mb*-TEPA and *Mb*-PEHA in THF determined by fluorescence quenching measurements.

Dispersant	# of unreacted secondary amines	Level of Modification
<i>Mb</i> -PIBSI-TEPA	1.21 ± 0.04	$60 \pm 1\%$
<i>Mb</i> -PIBSI-PEHA	1.13 ± 0.03	$70 \pm 1\%$

Adsorption of *b*-PIBSI Dispersants onto Carbon Black Particles. After having characterized the extent of EC modification applied to the *b*-PIBSI dispersants, the adsorption of the oil-soluble dispersants *b*-PIBSI-DETA, *b*-PIBSI-TEPA, *b*-PIBSI-PEHA, *Mb*-PIBSI-TEPA, and *Mb*-PIBSI-PEHA onto carbon black particles (CBPs) used as models for the ultrafine particles (UFPs) generated in engine oil was investigated in dodecane. Since the construction of adsorption isotherms always requires the knowledge of the quantity of unbound ligand, earlier reports used the absorption of a pH-indicator to determine the concentration of secondary amines, and thus dispersant molecules in the solution.^{18,19} But since pH-indicators are usually water-soluble weak acids or bases that cannot dissolve in hexane, the procedure required a change of solvent from hexane where the adsorption measurements were conducted

to THF where the unbound dispersant concentration was determined from the absorption response of the pH-indicator. This procedure also limited the choice of a workable apolar solvent since it needed to be evaporated off to be replaced by more polar THF where the pH indicator was soluble. By contrast, fluorescence of the succinimide groups of the dispersants offers a means to determine the concentration of unbound dispersant in the same solvent where the adsorption measurements were carried out, down to extremely low dispersant concentrations by taking advantage of the extraordinary sensitivity of fluorescence.

A number of precautions needed to be taken when conducting these fluorescence experiments. First, while absorption is an absolute measurement, fluorescence only provides quantitative information with respect to a reference. Consequently, all fluorescence measurements on dispersant solutions were benchmarked against the fluorescence signal of a standard which was a 2.8×10^{-5} M 1-pyrenemethanol solution in methanol that was degassed, sealed, and kept in the dark for the duration of these experiments. Second, a small fraction of the succinimide chromophore was found to photobleach upon irradiation in the spectrofluorometer. While photobleaching could not be detected after acquisition of a single fluorescence spectrum, repeated irradiation for successive acquisition of the fluorescence spectra led to a noticeable decrease in fluorescence intensity. Consequently, each dispersant solution was discarded after acquisition of its fluorescence spectrum.

Following this procedure, calibration curves were generated by plotting the fluorescence intensity of the solution normalized to that of the standard against the concentration of PIBSI dispersant. The calibration curves are shown in Figure S5. The slope of these lines could be used as a massic fluorescence coefficient (MFC) to retrieve the concentration of an unknown *b*-PIBSI dispersant. Table 5 lists the values of the MFCs

obtained for the *b*-PIBSI dispersants. As the secondary amine content of the spacer increased, the MFC decreased as expected since secondary amines were found to quench the succinimide fluorescence.²⁰ EC modification increased the MFC of the modified dispersants *Mb*-PIBSI-TEPA and *Mb*-PIBSI-PEHA to a level close to that of *b*-PIBSI-DETA. This result is reasonable since those two modified dispersants were found to retain one unreacted secondary amine (Table 4) making their secondary amine content similar to that of *b*-PIBSI-DETA.

Table 5. Summary of the massic fluorescence coefficients (MFC) calculated from steady-state measurements in dodecane. ($\lambda_{\text{ex}} = 360 \text{ nm}$)

Polymer	MFC (L. g ⁻¹)	Polymer	MFC (L.g ⁻¹)
<i>b</i> -PIBSI-DETA	16.6 ± 0.5		
<i>b</i> -PIBSI-TEPA	14.1 ± 0.2	<i>Mb</i> -PIBSI-TEPA	17.1 ± 0.0
<i>b</i> -PIBSI-PEHA	8.6 ± 0.1	<i>Mb</i> -PIBSI-PEHA	15.5 ± 0.7

The MFCs could be used to determine the concentration of unbound dispersants in the adsorption experiments which were conducted as follows. A 3 g/L dispersant solution was prepared in dodecane and masses of 0.01 to 0.4 g of CBPs were added to the solutions. The solutions were agitated at room temperature for 24 h, long enough for the solutions to reach equilibrium.¹⁸ The solids were then filtered through 0.2 μm Millipore Teflon filters and each sample was weighed to determine the solution volume from the known density of dodecane (0.78 g.mL⁻¹). The fluorescence emission of the *b*-PIBSI and *Mb*-PIBSI dispersant solutions were measured at 420 nm and it was converted to the concentration of unbound dispersant C_{eq}

using the corresponding MFC value. The amount of adsorbed dispersant at equilibrium per unit surface of CBPs (Γ) expressed in $\mu\text{mol}/\text{m}^2$ was calculated using Equation 6,

$$\Gamma = \frac{(C_0 - C_{\text{eq}}) \times V}{m \times A} \quad (6)$$

where C_0 and C_{eq} represent the initial dispersant concentration and the equilibrium concentration of unbound dispersant after adsorption, respectively, V is the volume of the solution, m is the mass of CBPs, and A ($= 764 \text{ m}^2/\text{g}$) is the surface area of the CBPs.¹⁸

Two concentration regimes could be identified for the adsorption isotherms of the *b*-PIBSI dispersants onto the CBPs as shown in Figure 5. At low C_{eq} , binding of dispersant molecules occurs at single sites on the CBPs surface. As those sites become occupied, additional surfactant molecules adsorb on top of already adsorbed dispersant molecules leading to multilayer coverage of the CBPs that is associated with the precipitous increase in Γ observed for larger C_{eq} values ($C_{\text{eq}} > 400 \text{ mmol}/\text{m}^3$) in Figure 5. Consequently, the binding equilibrium constant of the *b*-PIBSI dispersants onto single sites at the surface of CBPs could be determined from the analysis of the Γ values in the concentration regime corresponding to the low C_{eq} values.^{19,25}

The binding isotherms Γ of *b*-PIBSI-DETA, *b*-PIBSI-TEPA, and *b*-PIBSI-PEHA are shown in Figure 5 where Γ was plotted as a function of C_{eq} to study the contribution of the different polyamine spacers on adsorption. For all three dispersants, the adsorption isotherm or the amount of dispersant adsorbed onto the CBPs increased as more dispersant was added to the solutions. For a given concentration of free dispersant in dodecane, *b*-PIBSI-DETA had

the largest amount of dispersant adsorbed onto the CBPs, followed by *b*-PIBSI-TEPA and *b*-PIBSI-PEHA.

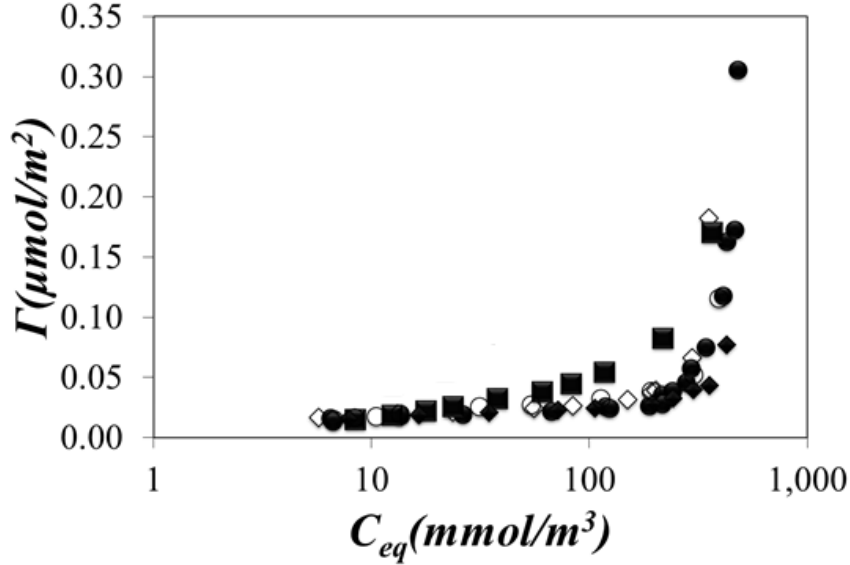


Figure 5. Adsorption isotherms in dodecane of (●) *b*-PIBSI-PEHA, (○) *Mb*-PIBSI-PEHA, (◆) *b*-PIBSI-TEPA, (◇) *Mb*-PIBSI-TEPA, and (■) *b*-PIBSI-DETA dispersants onto CB particles. [dispersant] = 3 g.L⁻¹

Comparison of the adsorption isotherms of the different PIBSI dispersants was conducted with the Langmuir model, which only handles the binding of the dispersants at low coverage of CBPs. To this end, Equation 7 was applied. In Equation 7, Γ_{\max} is the maximum amount of dispersant adsorbed per unit area and K is the binding constant of the adsorption process.

$$\Gamma = \frac{\Gamma_{\max} K C_{eq}}{1 + K C_{eq}} \quad (7)$$

Γ_{\max} and K were retrieved by rearranging Equation 7 into Equation 8. The simple Langmuir model could not fit the whole concentration range shown in Figure 5 for *b*-PIBSI-DETA, *b*-PIBSI-TEPA, and *b*-PIBSI-PEHA since multiple binding regimes were observed from the low to high end of the C_{eq} range. Therefore, Equation 8 was only used to fit the linear region of Figure 6A corresponding to the larger $1/C_{eq}$ values as shown in Figure 6B.

$$\frac{1}{\Gamma} = \frac{1}{\Gamma_{\max} K C_{eq}} + \frac{1}{\Gamma_{\max}} \quad (8)$$

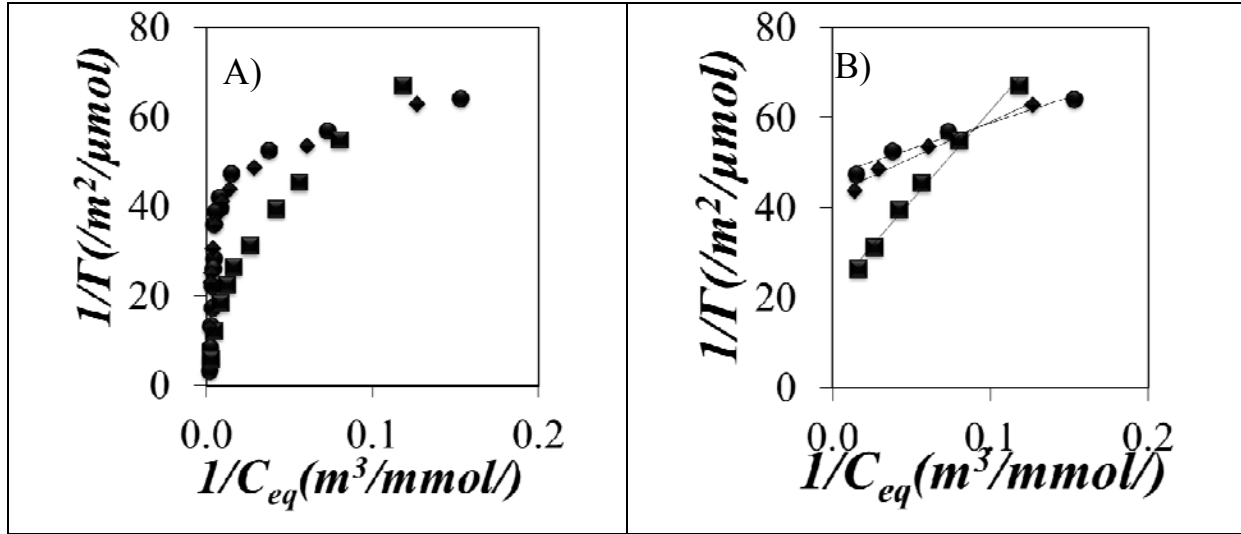


Figure 6. Plot of $1/\Gamma$ versus $1/C_{eq}$ over A) the entire range of dispersant concentrations and B) the linear part corresponding to the lower dispersant concentrations fitted to Equation 8 for (●) *b*-PIBSI-PEHA, (◆) *b*-PIBSI-TEPA, and (■) *b*-PIBSI-DETA dispersants in dodecane.

The Γ_{\max} and K values retrieved by fitting the data shown in Figure 6B with Equation 8 are listed in Table 6. The results indicate that the binding constant K increased strongly with the number of secondary amines in the polar core of *b*-PIBSI dispersants. The amount of dispersant needed to saturate the adsorption sites Γ_{\max} decreased with increasing number of

amines. Based on the K values, these trends indicate that the dispersants bind more strongly to the CBPs when the dispersants contain a higher number of secondary amines.

Table 6. Γ_{\max} and K values retrieved by fitting the data shown in Figures 6 and 7 with Equation 7.

Dispersant	Solvent	$\Gamma_{\max} \times 10^{10}$ (mol/m ²)	K (m ³ /mol)
<i>b</i> -PIBSI-DETA	dodecane	464 ± 29	54 ± 1
<i>b</i> -PIBSI-TEPA	dodecane	233 ± 6	268 ± 1
<i>b</i> -PIBSI-PEHA	dodecane	211 ± 6	412 ± 1
<i>Mb</i> -PIBSI-TEPA	dodecane	260 ± 1	239 ± 1
<i>Mb</i> -PIBSI-PEHA	dodecane	307 ± 8	130 ± 1

The binding isotherms of *b*-PIBSI-TEPA and *b*-PIBSI-PEHA were also compared to those given in Figure 7 for *Mb*-PIBSI-TEPA and *Mb*-PIBSI-PEHA, respectively. The results in Table 6 indicate that the binding constant K decreased for *b*-PIBSI-TEPA and *b*-PIBSI-PEHA after modification. Urethane groups were found to decrease the drive for *Mb*-PIBSI dispersants to adsorb on the surface of CBPs. Since *Mb*-PIBSI-PEHA had a higher fraction of modified secondary amines, the decrease was more pronounced for *Mb*-PIBSI-PEHA than for *Mb*-PIBSI-TEPA. The amount of dispersant needed to saturate the adsorption sites Γ_{\max} increased after modification. In effect, EC modification of *b*-PIBSI-TEPA and *b*-PIBSI-PEHA generated dispersants whose adsorption onto CBPs was more akin to that of *b*-PIBSI-DETA with smaller K and larger Γ_{\max} values compared to the values obtained with the non-modified dispersant analogues. Overall, these trends indicate that the binding of the

dispersants onto CBPs is more efficient before modification as expected, since the purpose of the modification is to decrease the basicity of the solution and not increase the ability of the dispersants to adsorb onto carbonaceous particulate matter.

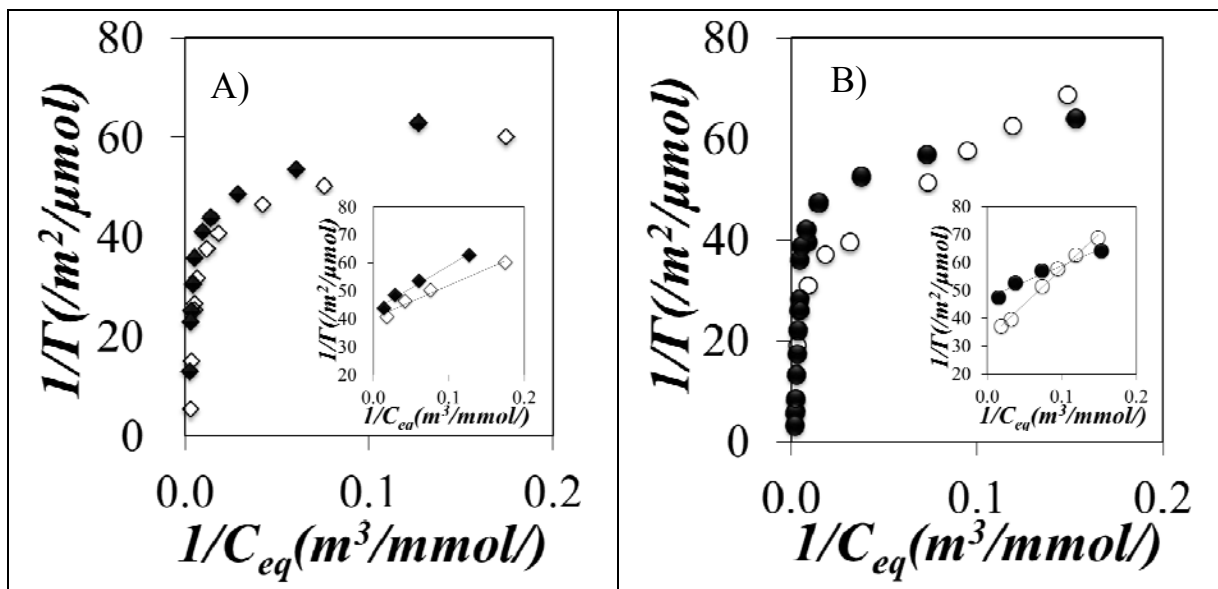


Figure 7. Plot of $1/\Gamma$ versus $1/C_{eq}$ for A) (\blacklozenge) *b*-PIBSI-TEPA and (\diamond) Mb-PIBSI-TEPA, and B) (\blacktriangle) *b*-PIBSI-PEHA and (Δ) Mb-PIBSI-PEHA dispersants in dodecane. Inserts: Linear part of the plot in Figures 7A) and B) corresponding to the lower dispersant concentrations fitted to Equation 8 for A) (\blacklozenge) *b*-PIBSI-TEPA and (\diamond) Mb-PIBSI-TEPA and B) (\blacktriangle) *b*-PIBSI-PEHA and (Δ) Mb-PIBSI-PEHA dispersants in dodecane.

CONCLUSIONS

Four *b*-PIBSI dispersants were prepared and the secondary amines in their polyamine core were modified by reaction with ethylene carbonate (EC). Successful modification of the dispersants was assessed by visual inspection of the ^1H NMR and FTIR spectra, but quantitative analysis of these spectra to extract the extent of secondary amine modification was complicated by inherent distortions of the spectra due to H-bonding between unreacted

secondary amines and succinimide carbonyls. The existence of unreacted secondary amines in the polyamine core of the *Mb*-PIBSI dispersants was unambiguously demonstrated by fluorescence measurements. As demonstrated in an earlier report,²⁰ secondary amines quench the fluorescence of succinimide groups very efficiently. However, quenching of succinimide moieties by urethane groups is much less efficient. Consequently, complete modification of secondary amines with EC was expected to result in a substantial increase in succinimide fluorescence for the *Mb*-PIBSI dispersants. This increase in fluorescence intensity would have been 216 and 271 % for *Mb*-PIBSI-TEPA and *Mb*-PIBSI-PEHA, respectively. Instead, a rather low 42 and 71 % increase in fluorescence intensity was observed for *Mb*-PIBSI-TEPA and *Mb*-PIBSI-PEHA, respectively. This result led to two conclusions. First, a substantial fraction α of secondary amines did not react with EC during the modification reaction. Second, fluorescence quenching experiments with the succinimide moieties should enable the determination of the level of modification of the *b*-PIBSI dispersants.

With this in mind, the fluorescence signal retrieved from the partially modified *Mb*-PIBSI dispersants was analyzed to account for the reduction in fluorescence quenching experienced by the succinimide pendants when secondary amines were replaced by urethane groups. This analysis took advantage of the similarity in chemical structure between small organic molecules (DEA and HEDBC) and the secondary amines and urethane species found in the polyamine linker. The Stern-Volmer (K_{sv}) constants obtained for the quenching of *N*-methyl succinimide by DEA and HEDBC were used to estimate the K_{sv} constant for the quenching of succinimide groups in *Mb*-PIBSI dispersants by urethane functions. In turn, this information was used to determine that 60 and 70% of the secondary amines of *b*-PIBSI-TEPA and *b*-PIBSI-PEHA had reacted with EC. This result was in good agreement with an

estimate of the level of secondary amine modification obtained by ^1H NMR assuming association of the *Mb*-PIBSI dispersants in solution. The partial reaction of the secondary amines was attributed to steric hindrance due to the presence of the bulky succinimide and urethane groups as well as H-bonding between secondary amine protons and succinimide carbonyls.

After having quantified the extent of modification in the *Mb*-PIBSI dispersants, their ability to adsorb onto the surface of carbon black particles (CBPs), used as mimics of the carbonaceous ultrafine particles (UFPs) found in engine oils, was compared to that of their unmodified analogs. The binding constants retrieved for the *Mb*-PIBSI dispersants were smaller than those of the unmodified dispersants suggesting that the modification had reduced their ability to act as colloidal stabilizers in oil. Together, these results illustrate that fluorescence quenching experiments can be employed to quantify the level of EC modification in *b*-PIBSI dispersants and how this modification affects the ability of dispersants to stabilize the UFPs generated in engine oils.

ACKNOWLEDGMENTS

The authors thank Imperial Oil and NSERC for their generous financial support of this research.

SUPPORTING INFORMATION AVAILABLE

FTIR and ^1H MNR spectra of PIBSA, *b*-PIBSI, and *Mb*-PIBSI dispersants, ^1H MNR spectra of dibutylamine (DBA) and 2-hydroxyethyl *N,N*-dibutylcarbamate (HEDBC), steady-state calibration curve of PIBSA, *b*-PIBSI, and *Mb*-PIBSI dispersants in dodecane and tables of pre-exponential factors and decay times retrieved from the analysis of the fluorescence decays

with a sum of exponentials. This information is available free of charge via the Internet at <http://pubs.acs.org>.

REFERENCES

- (1) Mortier, R. M.; Malcolm, F. F.; Orszulik, S. T. In *Chemistry and Technology of Lubricants*; Springer: London, 2009.
- (2) Jao, T. C.; Passut, C. A. In *Part D: Formulation, Surfactant Science Series*; Showell, M. S., Ed.; Handbook of Detergents; CRC Press, Boca Raton: Florida, 2006.
- (3) Barbadsz, E. A.; Lamb, G. D. Eds. In *Chapter 19: Additives for Crankcase Lubricant Applications*; Rudnik, L. R. Lubricant Additives: Chemistry and Application; CRC Press, Boca Raton: Florida, 2003; pp 458-490.
- (4) Gwinn, M. R.; Vallyathan, V. Nanoparticles: Health Effects-Pros and Cons. *Environ. Health Perspect.* **2006**, *114*, 1818-1825.
- (5) Tomlinson, A.; Danks, T. N.; Heyes, D. M.; Taylor, S. E.; Moreton, D. J. Interfacial Characterization of Succinimide Surfactants. *Langmuir* **1997**, *13*, 5881-5893.
- (6) Forbes, E. S.; Neustadter, E. L. The Mechanism of Action of Polyisobutenyl Succinimide Lubricating Oil Additives. *Tribology* **1972**, *5*, 72-77.
- (7) Le Suer, W. M.; Norman, G. R. Fire Resistant Hydraulic Fluid. USP 3272747, 1966.
- (8) Le Suer, W. M.; Norman, G. R. Reaction Product of High Molecular Weight Succinic Acids and Succinic Anhydrides with an Ethylene Polyamine. USP 3172892, 1967.
- (9) Stuart, A. F.; Orinda, R. G.; Anderson, N.; Drummond, A. Y. Alkenyl Succinimides of Tetraethylene Pentamine. USP 3202678, 1965.

- (10) Myers, D. In *Surfactant Science and Technology*; John Wiley & Sons: Hoboken, New Jersey, 2006.
- (11) Harrison, J. J.; Novara, C. Polymeric Dispersants Having Alternating Polyalkylene and Succinic Groups. USP 5112507, 1992.
- (12) Nalesnik, T. E.; Cusano, C. M. Dibasic Acid Lubricating Oil Dispersant and Viton Seal Additives. USP 4663064, 1987.
- (13) Wollenberg, R. H.; Rafael, S.; Plavac, F. Modified Succinimide. USP 4802893, 1989.
- (14) Wollenberg, R. H.; Rafael, S.; Plavac, F. Modified Succinimides. USP 4612132, 1986.
- (15) Mark, E. J.; Ermama, B.; Eirich, F. R. In *Science and Technology of Rubber*; Elsevier: The University of Akron, Akron, Ohio, 2005.
- (16) Tessier, M.; Maréchal, E. Synthesis of Mono and Difunctional Oligoisobutylenes-III. Modification of α -Chlorooligoisobutylene by Reaction with Maleic Anhydride. *Eur. Poly. J.* **1984**, *20*, 269-280.
- (17) Balzano, F.; Pucci, A.; Rausa, R.; Uccello-Barretta, G. Alder-Ene Addition of Maleic Anhydride to Polyisobutylene: Nuclear Magnetic Resonance Evidence for an Unconventional Mechanism. *Polym. Int.* **2012**, *61*, 1256-1262.
- (18) Shen, Y.; Duhamel, J. Micellization and Adsorption of a Series of Succinimide Dispersants. *Langmuir* **2008**, *24*, 10665-10673.
- (19) Dubois-Clochard, M. C.; Durand, J. P.; Delfort, B.; Gateau, P.; Barré, L.; Blanchard, I.; Chevalier, Y.; Gallo, R. Adsorption of Polyisobutenyl Succinimide Derivatives at a Solid-Hydrocarbon Interface. *Langmuir* **2001**, *17*, 5901-5910.

- (20) Pirouz, S.; Wang, Y.; Chong, J. M.; Duhamel, J. Characterization of the Chemical Composition of Polyisobutylene-Based Oil-Soluble Dispersants by Fluorescence. *J. Phys. Chem. B* **2014**, *118*, 3899-3911.
- (21) Chevalier, Y.; Dubois-Clochard, M. C.; Durand, J. P. Adsorption of Poly(Isobutenylsuccinimide) Dispersants at a Solid-Hydrocarbon Interface. *Prog. Colloid Polym. Sci.* **2001**, *18*, 110-114.
- (22) Won, Y.; Meeker, S. P.; Trappe, V.; Weitz, D. A. Effect of Temperature on Carbon-Black Agglomeration in Hydrocarbon Liquid with Adsorbed Dispersant. *Langmuir* **2005**, *21*, 924-932.
- (23) Phelan, J. C.; Sung, C. S. P. Fluorescence Characteristics of Cure Products in Bis(Maleimide)/Diallylbisphenol A Resin. *Macromolecules* **1997**, *30*, 6837-6844.
- (24) Kanaoka, Y.; Machida, M.; Ban, Y.; Takamitsu, S. Fluorescence and Structure of Proteins as Measured by Incorporation of Fluorophore. II. Synthesis of Maleimide Derivatives as Fluorescence-Labeled Protein-Sulfhydryl Reagents. *Chem. Pharm. Bull.* **1967**, *15*, 1738-1743.
- (25) Pucci, A.; Rausa, R.; Ciardelli, F. Aggregation-Induced Luminescence of Polyisobutene Succinic Anhydrides and Imides. *Macromol. Chem. Phys.* **2008**, *209*, 900-906.
- (26) Winnik, M. A.; Bystryak, S. M.; Liu, Z.; Siddiqui, J. Synthesis and Characterization of Pyrene-Labeled Poly(Ethylenimine). *Macromolecules* **1998**, *31*, 6855-6864.
- (27) Tomlinson, A.; Scherer, B.; Karakosta, E.; Oakey, M.; Danks, T. N.; Heyes, D. M.; Taylor, S. E. Adsorption Properties of Succinimide Dispersants on Carbonaceous Substrates. *Carbon* **2000**, *38*, 13-28.

Table of Content (TOC)

